Some Practical Aspects of Undulator Radiation Properties

Peter Ilinski,[1,2] Roger J. Dejus,[1] Efim Gluskin,[1] and Timothy I. Morrison[2]

Advanced Photon Source
Argonne National Laboratory
Argonne, IL 60439

[1] Advanced Photon Source, Argonne National Laboratory, Argonne, IL 60439
[2] Illinois Institute of Technology, Chicago, IL 60616

ANL/XFD/CP--90792
CONF-960848--21

ABSTRACT

It is important to be able to accurately predict the spectral and angular distribution of undulator radiation properties when designing beamlines at new synchrotron radiation facilities or when performing radiation experiments at already existing beamlines. In practice, the particle beam emittance and beam energy spread must be taken into account in modeling these properties. The undulators fabricated today are made with small RMS phase errors, making them perform almost as ideal devices. Calculation tools for numerical modeling of undulator radiation sources (ideal and nonideal) will be discussed, and the excellent agreement with experimentally obtained absolute spectral flux measurements of undulator A at the Advanced Photon Source verifies the high accuracy of the computer codes and the high quality of the undulators being built today. Our focus here is on flux properties useful in practical beamline designs, and the chosen examples demonstrate the versatility of computer programs available to beamline designers and experimentalists.

KEYWORDS:

Synchrotron radiation, insertion device, undulator radiation, numerical modeling, phase error, near-field effect, beam emittance, beamline design.

1. INTRODUCTION

The spectral and angular properties of undulator radiation are complicated, and several computer programs have been developed in recent years by various authors to cover most situations of practical interest.[1,2,3] At newly built synchrotron radiation facilities, these codes have become important tools for beamline design, undulator magnetic shimming, and accurate prediction of radiation characteristics in experimental setups. The starting point in beamline design for synchrotron radiation experiments involves an accurate description of the radiation source. Obviously, a complete beamline design includes many steps, however, in this paper we limit ourselves to software tools needed for calculation of undulator radiation source properties.

In almost all practical applications, the radiation can be considered to be emitted from an ideal source, i.e., an undulator with no magnetic field errors. The radiation emitted from one pole to the next is completely in phase, giving rise to perfect harmonics in the undulator spectrum. The main advantage of using this approach is a substantial reduction in computing time, and in most instances this approach will give a safe margin for the quantity being calculated. Further, undulator technology has been perfected in past years and the devices perform very close to ideal, providing justification for this approach. Today devices with very small RMS phase errors are fabricated and installed in storage rings around the world.[4,5,6]

Sometimes, however, it is important to be able to estimate the shape and intensity of the spectral harmonics of a real device. Therefore, the measured magnetic field profile of the undulator may also be used by some computer programs for an accurate prediction of the emitted radiation. The effect of a nonideal magnetic field on the spectrum is such that the higher harmonics of the radiation will diminish in intensity. The radiation properties are in practice also strongly influenced by the finite size and divergence (emittance) of the stored particle beam and the beam energy spread. These effects are, however, in general taken into account in both types of computer programs, i.e., codes using both ideal and measured magnetic field profiles.

DISCLAIMER

A useful set of programs, which calculate the radiation characteristics from ideal synchrotron radiation sources and the radiation interaction with optical elements, has been collected and is available under a common graphical user interface (GUI) called XOP (x-ray optics utilities).[7] Most of the experience gained and presented here have been obtained by using computer codes from XOP. The user friendly GUI makes the XOP codes a powerful tool not only for beamline designs but also for fast *in-situ* calculations to guide and verify experimental setups and conditions.

To demonstrate the capabilities of the tools, we have chosen to examine some of the radiation properties of undulator A at the Advanced Photon Source (APS). Our focus here is on flux properties useful in practical beamline designs. For example, the influence of the size of the aperture and its alignment in relation to the undulator axis on the spectrum and the effect of the beam emittance on the spectrum are presented. Further, to check the validity of the calculated spectra and the performance of the device, we have made comparisons with experimentally obtained spectra, and in all cases we have found excellent agreement with absolute flux measurements verifying the high accuracy of the computer codes (as well as the undulator performance).

2. UNDULATOR A SPECTRAL FLUX

Undulator A was optimized to provide high flux and continuous coverage over a wide energy range (3 - 50 keV) by utilization of the first, third and fifth harmonics of radiation (which was made possible because of the high magnetic quality of the device).[8,9] Undulator A is a planar hybrid device with 72 magnetic periods of 3.30 cm period length. For a single-particle (zero emittance), the radiated n^{th} harmonic energy is given by

$$E_n[keV] = \frac{0.95E^2[GeV]n}{\lambda_u[cm]\left(1 + K^2/2 + \gamma^2\theta^2\right)}, \qquad (1)$$

where E is the beam energy (7.0 GeV), $\gamma = 1957E[GeV]$, λ_u is the undulator period, $K = 0.934\lambda_u[cm]B_{eff}[T]$ is the deflection parameter, $B_{eff}[T]$ is the effective magnetic field (same as the peak field for an ideal sinusoidal magnetic field), and θ is the polar angle measured from the undulator axis. The tuning of the spectrum is achieved by changing the K value, which may be obtained in different ways. For undulator A, the magnetic gap is allowed to be changed. The useful range of gap settings for undulator A is 10.5 mm to 35.0 mm with K values ranging from 2.77 to 0.25.

In reality the radiation characteristics depend on the particle beam emittance and the beam energy spread. A typical spectrum for the flux through a 2.50 (h) x 1.00 (v) mm aperture at 30.0 m from the source is shown in Fig. 1, calculated for undulator A at a gap of 18.6 mm (K=1.20). We used the following measured beam parameters -- source size (x,y) and beam divergence (x',y') (obtained at a current of 20 mA) [10]

$$\sigma_x = 300 \pm 25\mu m \qquad \sigma_{x'} = 25 \pm 2.5\mu rad$$
$$\sigma_y = 60 \pm 9\mu m \qquad \sigma_{y'} = 5.3 \pm 0.5\mu rad\ .$$

The corresponding horizontal (x) and vertical (y) emittances are

$$\varepsilon_x = 7.5 \pm 0.6 \times 10^{-9}\, m \cdot rad \qquad \varepsilon_y = 3.2 \pm 0.6 \times 10^{-10}\, m \cdot rad\ ,$$

and the coupling constant χ, which is the ratio of the vertical to the horizontal emittance, becomes $4.3 \pm 1.3\%$. We used the design value of 0.1% for the value of the standard deviation of the storage ring beam energy spread.

The intense first harmonic appears at 8.1 keV, which is slightly lower than the value predicted from Eq. (1) due to the beam emittance. The peaks are also broadened due to the beam emittance and the beam energy spread. The relatively intense and broad even harmonics seen in the spectrum are purely an effect of the beam emittance and the angular acceptance of the aperture for an ideal device.

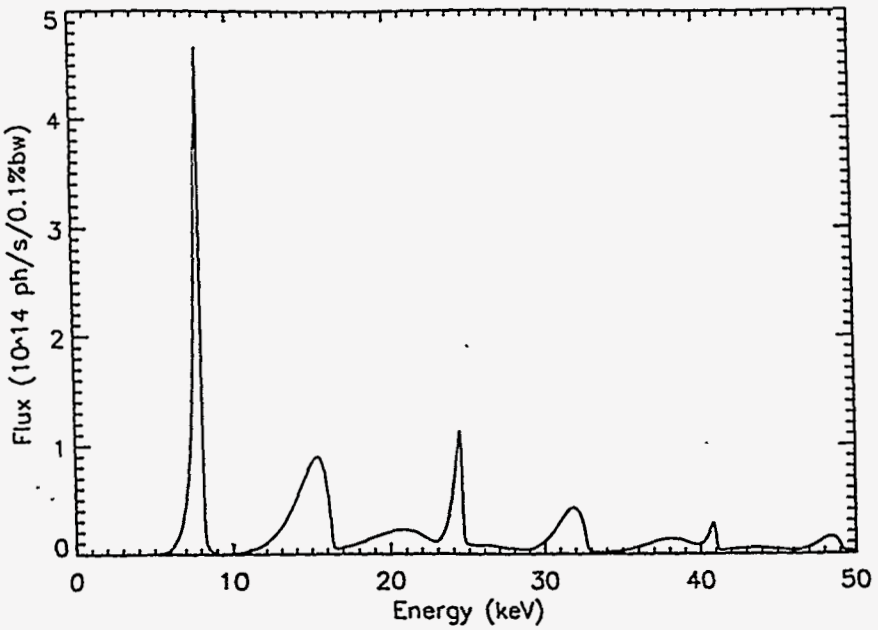

Fig. 1. Undulator A flux for a 2.50 (h) x 1.00 (v) mm aperture at 30.0 m from the source. The K value is 1.20, and the beam parameters are $\sigma_x = 300$ μm, $\sigma_y = 60$ μm, $\sigma_{x'} = 25$ μrad, $\sigma_{y'} = 5.3$ μrad, and $\sigma_E / E = 0.1\%$. The beam energy is 7.0 GeV and the beam current is 100.0 mA.

The undulator radiation characteristics from the experimentalists' point of view are defined by a set of fixed parameters, such as the storage ring beam energy, the horizontal and vertical emittances, the storage ring beam energy spread, and the undulator period length, and by a set of parameters that are subject to change. The undulator gap and the beamline geometry, e.g., the aperture accepting the undulator radiation may be varied directly by the experimentalists. An increased size of the acceptance aperture increases the peak flux but also the harmonic width, as is seen in Fig. 2. Similarly, Fig. 3 shows the effect of different aperture sizes on the linear polarization amount (Stokes parameter $S1$). A large aperture size degrades the linear polarization amount on both the high and low energy side of the harmonic energy, but, as seen in Figure 3, a linear polarization amount of 98% or higher is expected at energies where there is a reasonably high flux.

The flux at the harmonic energies will increase rapidly up to an angle that is approximately $\sqrt{\sigma^2_{x',y'} + \sigma^2_{r'}}$, where $\sigma_{r'} \sim \frac{1}{2\gamma}\sqrt{\frac{1+K^2/2}{nN}}$ is the undulator radiation natural divergence at the harmonic energies, and $\sigma_{x',y'}$ is the beam angular divergence. The spatial distribution of the radiation for a selected harmonic energy is easily calculated with the undulator radiation program and may be used to determine an appropriate size of the acceptance aperture to cover the radiation contained in the central cone. The size of the central cone of radiation is approximately 2.50 (h) x 1.00 (v) mm at 30.0 m from the source for the first odd harmonics, and this is the reason for maintaining the aspect ratio of 2.5:1.0 for all selected apertures.

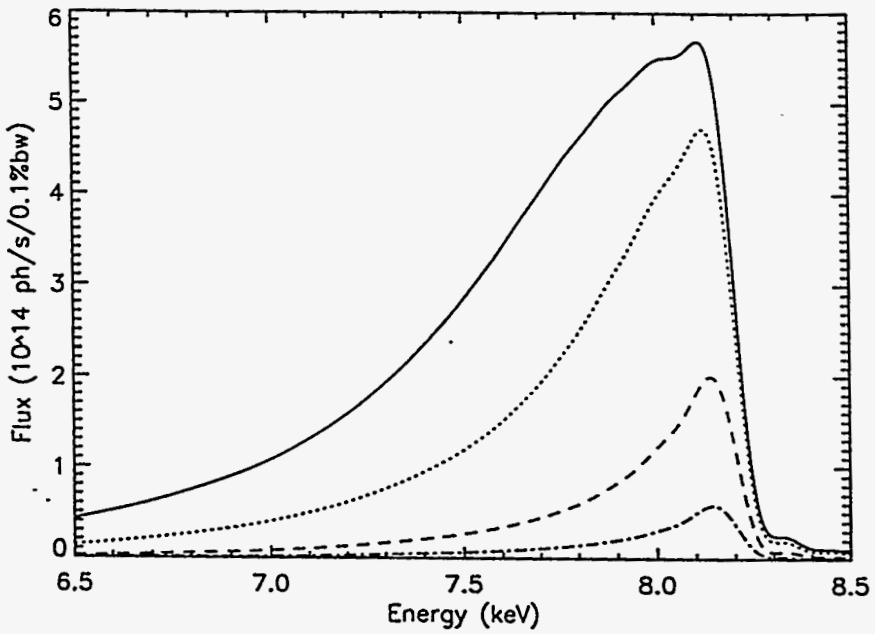

Fig. 2. First harmonic radiation around 8.1 keV for undulator A for four apertures at 30.0 m from the source. K=1.20 and other beam parameters as in Figure 1. (——) 3.75 x 1.50 mm, (·····) 2.50 x 1.00 mm, (- - -) 1.25 x 0.50 mm, (- · - ·) 0.625 x 0.250 mm.

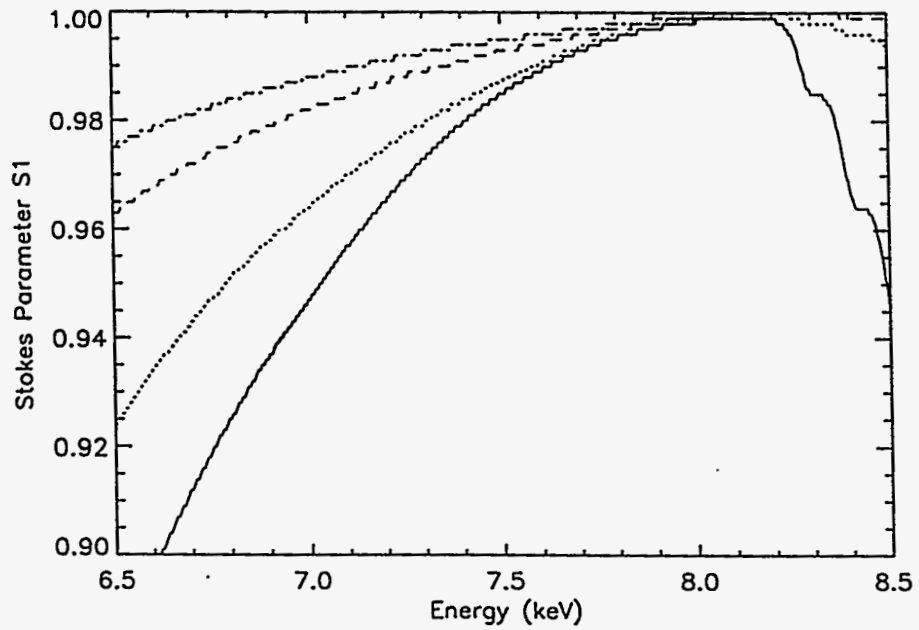

Fig. 3. Stokes parameter *S1* around 8.1 keV for undulator A for four apertures at 30.0 m from the source. K=1.20 and other beam parameters as in Figure 1. (——) 3.75 x 1.50 mm, (·····) 2.50 x 1.00 mm, (- - -) 1.25 x 0.50 mm, (- · - ·) 0.625 x 0.250 mm.

The natural width of the undulator radiation, the beam emittance and beam energy spread, and the size of the aperture all contribute to the width of the harmonic peak. The width can be estimated by

$$\frac{\Delta E}{E} \sim \sqrt{\left(\frac{1}{nN}\right)^2 + \left(\frac{(\gamma\sigma_{x'})^2 + (\gamma\sigma_{y'})^2 + (\gamma\theta_{ap,x})^2 + (\gamma\theta_{ap,y})^2}{1+K^2/2}\right)^2 + \left(2\frac{\Delta\gamma}{\gamma}\right)^2}\ , \qquad (2)$$

where $\Delta\gamma/\gamma$ is the FWHM of the beam energy spread, $\theta_{ap,x,y}$ is the aperture half-angle, and N is the number of undulator periods. The beam energy spread will result in symmetrical broadening, while the emittance will cause a broadening only on the low energy side of the peak. The beam energy spread will cause a noticeable broadening only for high order harmonics (high energies) when using small apertures. We notice that the width increases almost quadratically with increasing undulator harmonic energy when the aperture is the dominant term. The width varies substantially with the experimental conditions, and a wide peak can be obtained by selecting a large aperture. However, an increase of the angular acceptance will reduce the energy resolution when using a crystal monochromator.

Sometimes the exact shape of the angular distribution of the radiation at fixed energies is important. In this regard, it is important to realize that the angular distribution is not necessarily peaked at the center of the radiated beam. The emittance of the particle beam smears the radiation pattern and broadens the peaks unevenly in the horizontal and vertical direction. In the horizontal direction, the radiation is generally peaked on-axis because of the relatively large emittance in this direction, however, for the vertical distribution, it is quite different, and the maximum in the angular distribution will appear off-axis at an angle that is approximately

$$\theta = \frac{1}{\gamma}\sqrt{\frac{0.95E^2[GeV]n}{E_n[keV]\lambda_u[cm]} - (1+K^2/2)}\ , \qquad (3)$$

which follows from Eq. (1). Fig. 4 shows vertical distributions (centered in the horizontal direction) at the energy of the peak of the first harmonic, and at two energies below the harmonic energy. The ratio of the peak-to-valley intensity can be quite large when energies substantially below the harmonic energy are used, thus illuminating a sample or an optical element unevenly.

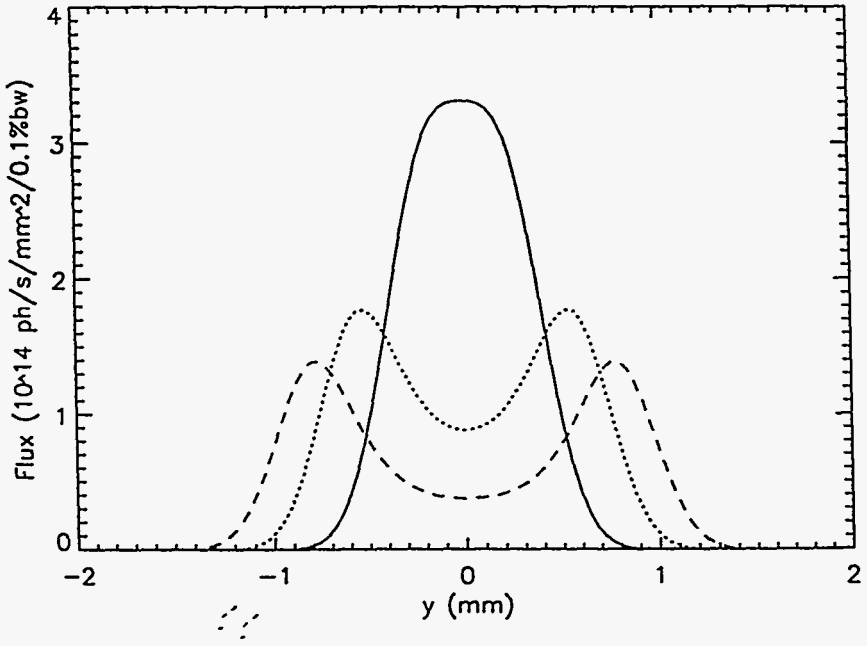

Fig. 4. Vertical radiation profiles for undulator A at and below the first harmonic energy of 8.1 keV at 30.0 m from the source. K=1.20 and other beam parameters as in Figure 1. (——) 8.10 keV, (·····) 7.80 keV, (- - -) 7.50 keV.

3. UNDULATOR A FLUX TUNING CURVES

The flux tuning curves are obtained by tracing the peak intensities of the harmonics versus energy when changing the *K* parameter (for undulator A, the magnetic gap is changed). The flux tuning curves calculated for an ideal device, for a series of aperture sizes, are shown in Fig. 5, and the full width at half maximum (with no baseline subtraction) of the same harmonics is presented in Fig. 6.

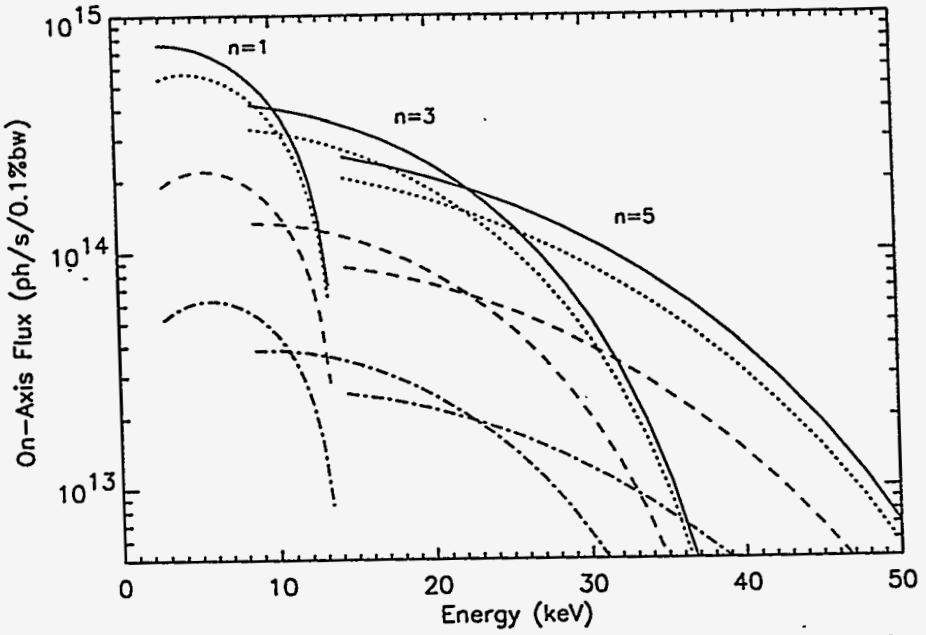

Fig. 5. On-axis flux tuning curves for the first (n=1), third (n=3), and fifth (n=5) harmonics of radiation for undulator A for four apertures at 30.0 m from the source. Beam parameters as in Figure 1. (——) 3.75 x 1.50 mm, (·····) 2.50 x 1.00 mm, (- - -) 1.25 x 0.50 mm, (- · - ·) 0.625 x 0.250 mm.

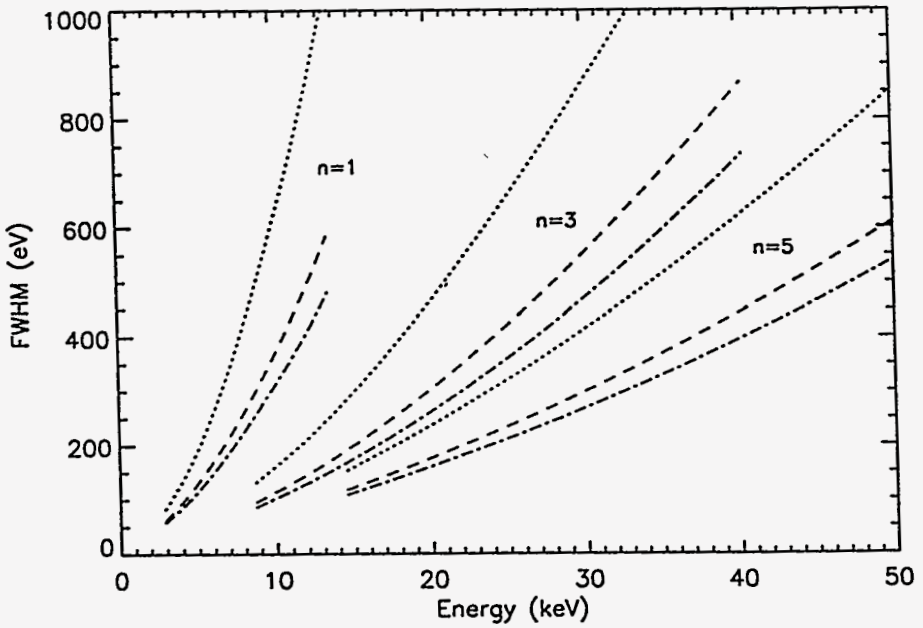

Fig. 6. On-axis tuning curves for the full width at half maximum (FWHM) for the first (n=1), third (n=3), and fifth (n=5) harmonics of radiation for undulator A for three apertures at 30.0 m from the source. Beam parameters as in Figure 1. (·····) 2.50 x 1.00 mm, (- - -) 1.25 x 0.50 mm, (- · - ·) 0.625 x 0.250 mm.

As before, the calculations were made using a coupling constant of 4.3% and a beam energy spread of 0.1%. The largest aperture size (3.75 x 1.50 mm at 30.0 m) clearly extends beyond the central cone of radiation as seen in the relatively small incremental increase in flux in comparison with the next smaller size aperture (2.50 x 1.00 mm). The finite size of the apertures contributes significantly in all cases to the broadening of the harmonics (the 3.75 x 1.50 mm aperture introduces a large baseline intensity, and was omitted from Figure 6).

In earlier work,[11] we compared the measured absolute spectral flux from undulator A with simulations using the code UR (see reference 2), which uses the measured undulator magnetic field as input to calculate the radiated spectra. The results were very gratifying since we observed a remarkably good agreement between the experimental results and the calculations. Fig. 7 shows a comparison of experimentally obtained tuning curves[12] and calculated tuning curves[13] assuming an ideal undulator. The measurements were made at two different beam emittances with different coupling constants. For small undulator gaps, the coupling constant was 8.5% and for large gaps 4.6%. The error bars were estimated to be at the 10% level with the main contributions discussed in previous work (reference 11).

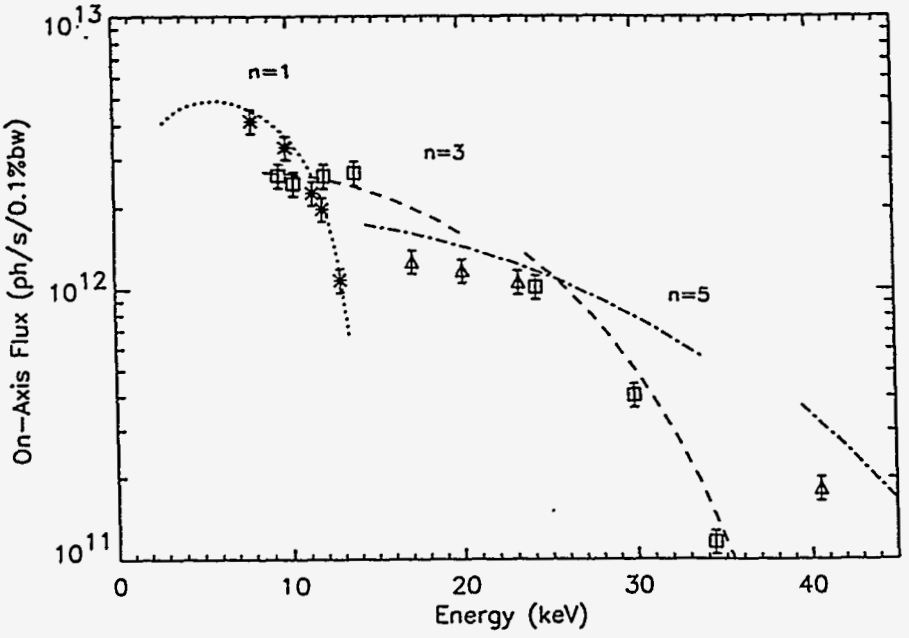

Fig. 7. Comparison of experimental results versus calculations for on-axis flux tuning curves for the first (·····), third (- - -), and fifth (- · - ·) harmonics of radiation for undulator A using an aperture of 150x75 μm located at 28.9 m from the source. There are two calculated curves for the third and fifth harmonics because of different coupling constants (8.5% for small undulator gaps and 4.6% for large gaps). Experimental results are for the first harmonic (*), third harmonic (□), and fifth harmonic (Δ) of radiation and were normalized to a beam current of 100.0 mA. The error bars are ± 10%.

The discrepancy between the measurements and the calculations can be attributed to the magnetic field errors of the real device, which cause the intensity of the higher harmonics to be reduced from the ideal. The anticipated reduction is most easily obtained by numerical simulations using the code UR for the practical case of including the beam emittance, the beam energy spread, and a finite size aperture. Results of such simulations indicate that we expect to obtain at least 90% of the ideal intensity for the third harmonic and at least 80% of the fifth harmonic for small apertures (~ 0.625 x 0.250 mm at 30.0 m from the source) using undulator A type devices at the APS. The corresponding figures for a large aperture (~ 2.50 x 1.00 mm at 30.0 m from the source) are approximately 95% and 90% for the third and fifth harmonic, respectively.

In the case of zero emittance, it has been shown that for a well-optimized undulator, the on-axis angular flux density for the odd harmonics is expected to vary according to the formula $I_0 e^{-(n\sigma_\phi)^2}$, where σ_ϕ is the RMS phase error, and n is the harmonic number.[14,15] Our experience from this work and on a prototype undulator,[16] indicates that the reduction is less than predicted from this formula when using a real beam and a finite size aperture.

In the future, improvements in the operation of the APS storage ring are expected to reduce the coupling constant to a value of 1.0% or smaller. The reduction is particularly important for brilliance-demanding experiments. To study the effect of the smaller coupling constant on flux, a comparison of tuning curves for two values of the coupling constant (4.3% and 1.0%) and two apertures is shown in Fig. 8. The flux increases for both aperture sizes for a smaller coupling constant, but the effect is not nearly as noticeable for the large aperture, confirming that experiments demanding small beam sizes would gain the most from such a reduction.

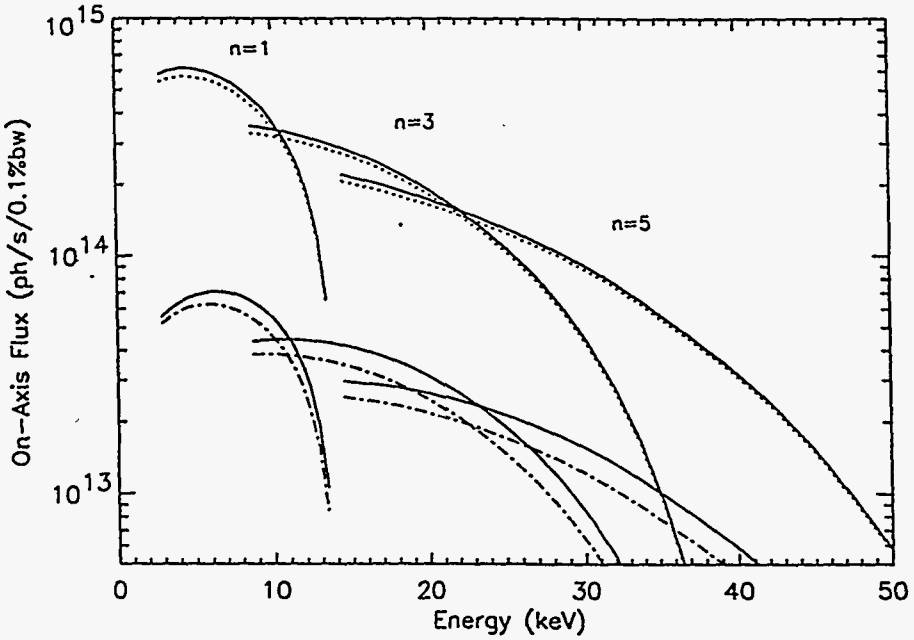

Fig. 8. On-axis flux tuning curves for the first (n=1), third (n=3), and fifth (n=5) harmonics of undulator A radiation for two apertures at 30.0 m from the source for different coupling constants χ at a beam current of 100.0 mA. (·····) 2.50 x 1.00 mm using χ=4.3% and adjacent solid curve (——) using χ=1.0%, (- · - ·) 0.625 x 0.250 mm using χ=4.3% and adjacent solid curve (——) using χ=1.0%.

4. OFF-AXIS CONDITIONS

Undulator radiation experiments may require situations when the aperture is not positioned on axis of the beam or a similar condition may occur because of misalignment of the aperture or missteering of the particle beam. The calculated change of the undulator spectrum for two apertures when moving the center of the aperture off-axis 0.25 mm in the vertical plane at 30.0 m from the source is shown in Fig. 9. Calculations were made for an ideal undulator in the far-field approximation, which assumes that the distance to the source is large compared to the length of the undulator. The validity of this approximation may be expressed by the near-field parameter introduced by Walker[17]

$$W = \frac{L^2\theta^2}{2\lambda D}, \qquad (4)$$

where L is the length of the undulator, D is the distance to the observation point, θ is the observation angle, and λ is the radiated wavelength.

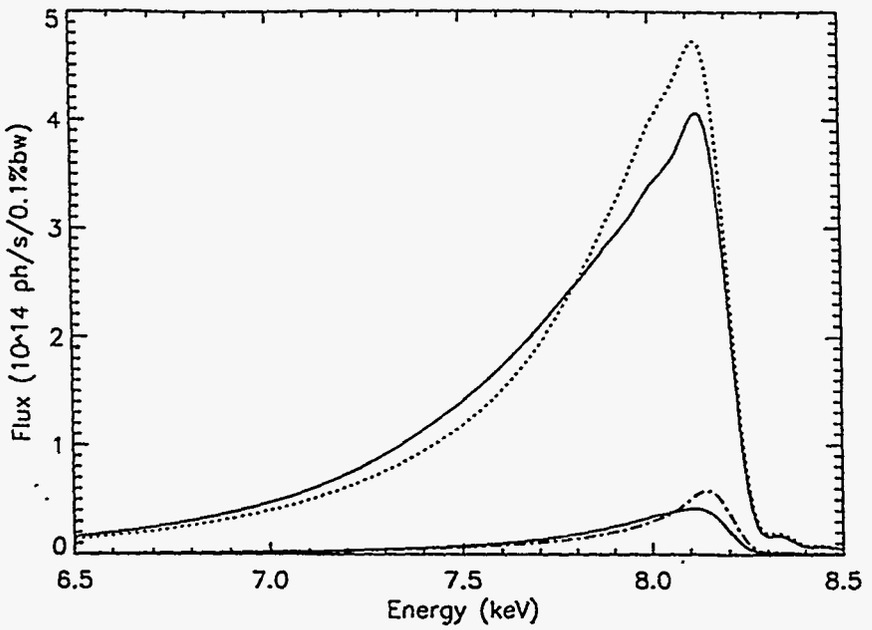

Fig. 9. Undulator A flux for two apertures for on- and off-axis positions at 30.0 m from the source. K=1.20 and other beam parameters as in Figure 1. (·····) 2.50 x 1.00 mm on-axis and adjacent solid curve (——) for a vertical offset of 0.25 mm, (- · - ·) 0.625 x 0.250 mm on-axis and adjacent solid curve (——) for a vertical offset of 0.25 mm.

Taking the finite distance into account may lead to an energy broadening of the harmonics, depending on the value of the off-axis angle. The estimated harmonic broadening due to the near-field effect is

$$\frac{\Delta E}{E} \sim \frac{W}{nN}, \tag{5}$$

which is W times broader than the natural width $1/nN$. Thus, $W \geq 1$ may be taken as a criterion when the near-field effect is expected to be observed. For the case of undulator A at an energy of 8.1 keV (L=2.4 m, D=30.0 m) for $\gamma\theta = 0.5$ (1.1 mm off-axis at 30.0 m from the source), the near-field parameter W is 0.8, and, for $\gamma\theta = 0.7$ (1.5 mm off-axis at the same distance), W is 1.6. The far-field approximation is expected to be valid in the first case, but the finite distance should be noticeable in the second case, causing the monochromatic intensity to decrease by a factor of $1/2W$. Despite the fact that the near-field effect will decrease the intensity at a particular energy, the total intensity radiated at a given angle should not change. The finite particle beam emittance also broadens the undulator harmonics and decreases the intensity. The emittance broadening will dominate over the near-field effect for off-axis angles smaller than $4\sigma_{x',y'} D/L$.[18] For the given emittance (with 4.3% coupling) and setup parameters, this angle is 265 μrad (8.0 mm off-axis at 30.0 m from the source) in the vertical direction and 1250 μrad (37.5 mm off-axis at the same distance from the source) in the horizontal direction. Thus, the near-field effect is not important for the cases described above and the far-field approximation is still valid.

5. DISCUSSION

In this paper we have presented a few typical examples related to undulator radiation properties that are of general practical interest to beamline designers and experimentalists. In particular the codes under the graphical user interface XOP have been proven useful during beamline designs and for calculation of undulator radiation characteristics. The computer codes can be obtained by contacting the author (RJD).

6. ACKNOWLEDGMENTS

This work was supported by the U.S. Department of Energy, BES-Materials Sciences, under contract No. W-31-109-ENG-38.

7. REFERENCES

[1] R.P. Walker and B. Diviacco, "*URGENT - A computer program for calculating undulator radiation spectral, angular, polarization, and power density properties,*" Rev. Sci. Instrum. 63 (1), pp. 393-395, 1992.

[2] Roger J. Dejus and Alfredo Luccio, "*Program UR: general pupose code for synchrotron radiation calculations,*" Nucl. Instr. and Meth., A347, pp. 61-66, 1994.

[3] P. Elleaume and X. Marechal, "*B2E, A software to compute synchrotron radiation from magnetic field data, version 1.0,*" ESRF-SR/ID-91-54, 1991.

[4] S.C. Gottschalk, K.E. Robinson, I. Vasserman, R. Dejus, and E.R. Moog, "*End Field Design and Tuning Methods for Insertion Devices,*" proceedings of national conference on synchrotron radiation and instrumentation, SRI-95, Rev. Sci. Instrum. 67 (9), 1996, in press.

[5] Joel Chavanne and Pascal Elleaume, "*Insertion devices at the ESRF,*" Rev. Sci. Instrum. 66 (2), pp. 1868-1871, 1995.

[6] R.P. Walker, R. Bracco, A. Codutti, B. Diviacco, D. Millo and D. Zangrando, "*Status of ELETTRA Insertion Devices,*" proceedings of the U.S. Particle Accelerator Conference, May 1-5, 1995.

[7] Roger J. Dejus and Manuel Sanchez del Rio, "*XOP: A graphical user interface for spectral calculations and x-ray optics utilities,*" proceedings of national conference on synchrotron radiation and instrumentation, SRI-95, Rev. Sci. Instrum. 67 (9), 1996, in press.

[8] B. Lai, A. Khounsary, R. Savoy, L. Moog, and E. Gluskin, "*Undulator A Characteristics and Specifications,*" Argonne National Laboratory Report, ANL/APS/TB-3, February 1993.

[9] Roger J. Dejus, Barry Lai, Elizabeth R. Moog, and Efim Gluskin, "*Undulator A Characteristics and Specifications: Enhanced Capabilities,*" Argonne National Laboratory Report, ANL/APS/TB-17, May 1994.

[10] P. Ilinski, ANL, unpublished information, 1996.

[11] Z. Cai, R. J. Dejus, P. Den Hartog, Y. Feng, E. Gluskin, D. Haeffner, P. Ilinski, B Lai, D. Legnini, E.R. Moog, S. Shastri, E. Trakhtenberg, I. Vasserman, and W. Yun, "*APS Undulator Radiation - First Results,*" proceedings of national conference on synchrotron radiation and instrumentation, SRI-95, Rev. Sci. Instrum. 67 (9), 1996, in press.

[12] See reference 10.

[13] Roger J. Dejus, ANL, computer program TCAP (based on the Bessel function approximation), unpublished, 1996.

[14] Bruno Diviacco and Richard P. Walker, "*Recent advances in undulator performance optimization,*" Nucl. Instr. and Meth., A368, pp. 522-532, 1996.

[15] R.P. Walker, "*Interference effects in undulator and wiggler radiaton sources,*" Nucl. Instr. and Meth., A335, pp. 328-337, 1993.

[16] Roger J. Dejus, Isaac Vasserman, Elizabeth R. Moog, and Efim Gluskin, "*Phase errors and predicted spectral performance of a prototype undulator,*" Rev. Sci. Instrum. 66 (2), pp. 1875-1877, 1995.

[17] R.P. Walker, "*Near field effects in off-axis undulator radiation,*" Nucl. Instr. and Meth., A267, pp. 537-546, 1988.

[18] D.A. Mossessian and P.A. Heimann, "*Characterization of ALS Undulator Radiation - high K, Taper, and the Near Field Effect,*" Rev. Sci. Instrum. 66 (11), pp. 5153-5161, 1995.